Realisation of a biocompatible diffraction grating using an ArF excimer laser

Realisation of a biocompatible diffraction grating using an ArF excimer laser

Abdulsattar. A. Aesa[1] and C. D. Walton[2]
[1]Department of Physics, College of Education/Al-Hawija, University of Kirkuk, Iraq
E-mail: a_aesa@uokirkuk.edu.iq
[2]School of Mathematics and Physical Sciences, University of Hull, UK, HU6 7RX

Abstract. We report the fabrication of a bio-compatible diffraction grating made out chitosan, a derivative of chitin. The diffraction grating has been realised by laser ablation using 193 nm excimer laser. Thin spun coated chitosan films 520 nm thick were used in the laser ablation experiments. We report a laser ablation threshold for chitosan of F_T = 85 ± 8 mJcm^{-2}. A clean laser ablation process is observed with very little material redeposited on the sample. Following equipment; white light interferometry, scanning electron microscopy, power spectral density and Fraunhofer diffraction measurements were utilized to characterise the diffraction grating. Calculation of the temperature rise induced during laser ablation has been carried out and compared with decomposition temperatures deduced from thermogravimetric data. Applications of bio-compatible gratings realised by laser direct write patterning are briefly discussed.

Keywords: diffraction grating, excimer laser, laser ablation, chitosan

1. Introduction

There is a great deal of interest in diffraction gratings made from bio-compatible materials within the scientific community. Interestingly, one of the earliest reported amplitude grating was realised by Rittenhouse as far back as 1786. The grating consisted of a thin taught wire formed around two fine pitch brass screws. It would appear the grating was not used for scientific purposes, however, Fraunhofer reproduced a similar grating in about 1813 using the first-ever ruling engine [1]. Diffraction gratings can be classified as *amplitude* gratings as in the latter example and *phase* gratings. When an electromagnetic wave is an incident on a diffraction grating it will have its electric field amplitude, or phase, or both, modified. Both types of gratings have been fabricated by lasers for many years, however, as new material is developed new applications also emerge. As a result, Several different techniques for creating diffraction gratings are now usable including; Mechanical scripting[1], dip-pen lithography[2], 3D printing[3], micro-contact printing[4,5] and laser ablation[6–8] to name a few. In this work, we report using a laser direct write (LDW) method to fabricate surface relief grating. A DLW method is useful in many areas of science and technology as gratings can be written at specific spatial locations on a device architecture. An area of specific interest in this work is the realisation of bio-compatible diffraction gratings for lab-on-chip (LOC) sensors.

We report laser ablation of spun coated chitosan thin films realised by (DLW) using short ultraviolet wavelength emitted by a 193nm ArF pulsed laser. This fabrication route has an advantage over some processes. It is a relatively quick processing technique as the workpiece can be rapidly translated relative to a stationary beam or one can use scanning mirrors to steer a laser beam over a stationary sample or a combination of both. The LDW method, therefore, complements other fabrication methods that are used to produce working LOC sensors or devices [9]. LOC architectures often integrate fluidic channels, lenses, lens arrays, gratings, textured hydrophobic surfaces all of which have been realised by laser patterning [10]. It is therefore important to establish the optimum laser parameters and conditions that are required to fabricate bio-compatible optical components. This includes identifying laser ablation removal rates, the laser ablation threshold and to understand and often minimise laser induced surface roughness of optical components. Optical absorption of a laser beam and hence depth resolution is dependent on the laser wavelength where the former increases with decreasing laser wavelength. Therefore, ultraviolet (UV) and vacuum ultraviolet (VUV) lasers are an ideal choice for achieving high depth resolution during laser processing. There are many examples (and references within) of UV and VUV in the literature reporting ablation patterning that covers a range of laser emission wavelengths: Krypton Fluoride (KrF) 248nm [11], Argon Fluoride, (ArF) 193nm [12] and VUV Fluorine (F2) 157nm [13]. In addition to optimising depth resolution, it is often desirable to reduce the footprint of LOC sensors and devices and consequently there is also a need to achieve high lateral spatial resolutions. Generally, this is addressed using high numerical aperture lenses, where the lateral resolution is given as $R = k\lambda / NA$, where λ is the laser wavelength, NA is the numerical aperture of the lens and *k* is material dependent constant. Therefore, large numerical aperture lenses and short-wavelength are key when realising small and compact features. There are many objective lenses that meet these criteria for high-resolution laser processing such as multi-element refractive lenses or using reflective Schwarzschild objectives. We note this work is not primarily looking at achieving sub-micron features but what is of more importance at this stage is to report the behaviour of chitosan when subjected to UV laser radiation.

Chitosan has been taken high attention of scientific researchers as a bio-compatible material for many applications [14]. the chemical structure of chitosan is shown in figure 1, which is a natural polymer (polysaccharide) prepared from chitin by deacetylation.

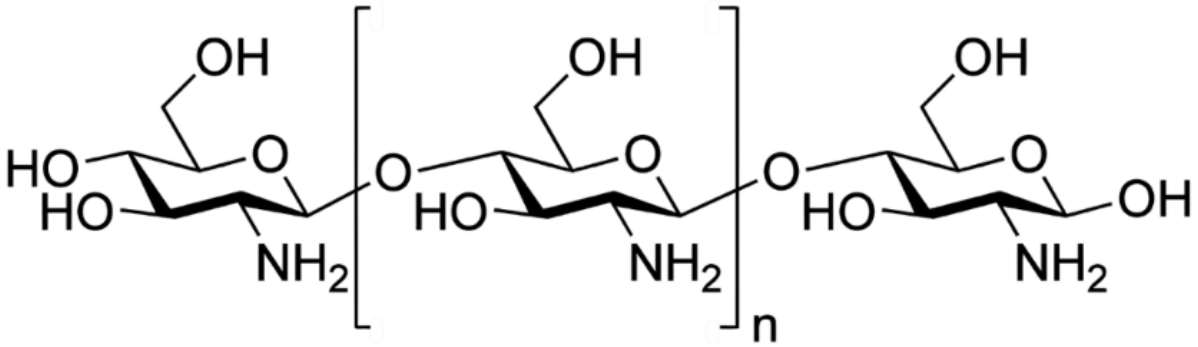

Figure 1: Chitosan chemical structure.

Chitosan can be easily spun to make thin films that are made available in planar form for laser processing. It is a material that has been employed to be used for wide range of applications, for example, medical, pharmaceutical, for example, it can be used to a substitute for artificial skin [15], bandages and contact lenses [16], drug delivery vehicles [17] surgical sutures [18,19], and to make waveguides for routing light around LOC architectures [20].

2. Experimental

Laser processing has been carried out using a 193nm excimer laser (Lambda Physik LPF 202). Figure 2 illustrates the experimental set-up for the laser processing work was used to realise the diffraction grating the scope of this paper.

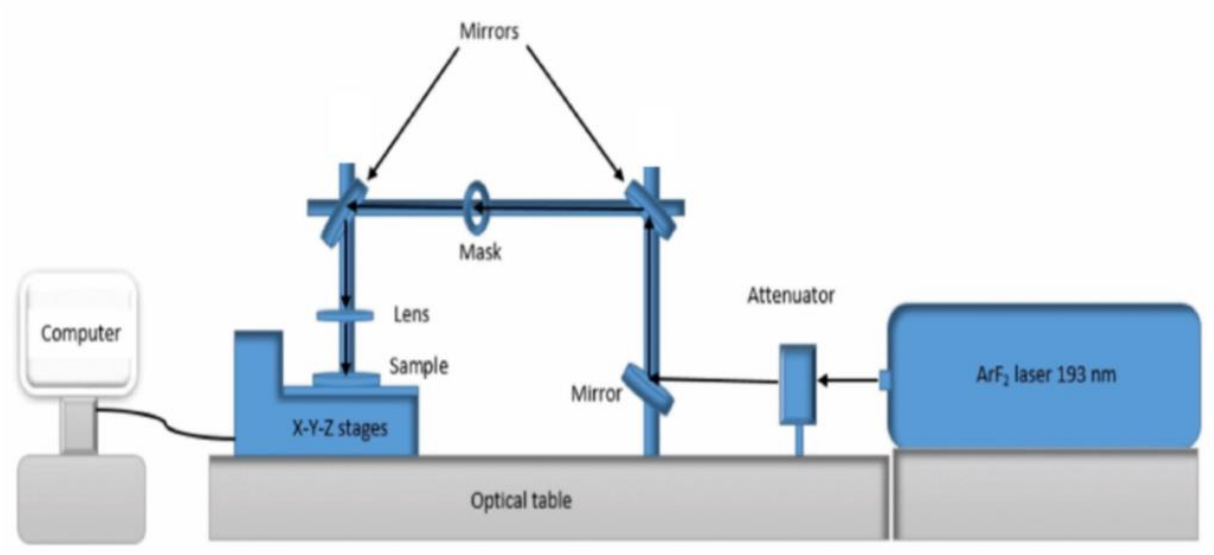

Figure 2: Schematic of the beam delivery system of the 193nm excimer laser.

An object mask was used as a parallel bar TEM grid (Agar co, 3.05 mm diameter 400 Parallel Bar Nic kel: AGG2016N). To pick the most homogeneous portion of the beam, the grid was positioned in the raw beam. × 1/5 magnification was used to image the mask onto the surface of the chitosan film. The laser ablation chitosan grating was characterized by the following instruments; Optical Microscope (Leica DMLM), White Light Interferometer (WLI, WYKO NT1100), and Scanning Electron Microscopy (SEM, Zeiss EVO60). During the fabrication process of the grating, all processed samples were translated relative to the laser beam using a nano motion control stages (Aerotech Fibre Align). To control the laser fluence, the laser output was passed through a double rotating plate attenuator (Metrolux, ML2110). Dielectric mirrors designed for 45 degrees transmission were used to direct the beam in a vertical direction to the specimen. This sample was oriented in a horizontal position, chosen for ease of sample positioning and a practical reason for laser processing of liquid samples. Joule meter (Molectron) and a fast photodiode (Hamamatsu, S7911) connected to an oscilloscope (Infinium, 500MHz, 2 Gb Samples s^{-1}) were utilised to measure the output energy and the temporal shape of the ArF 193 nm excimer laser respectively. The diffracted order efficiencies were measured using a large area detector (CASCO silonex- SLSD-71N5) and a 5 Watt HeNe laser (model, 1125P)

2.1. Sample Preparation

Chitosan (Chitosan-448869) as a powder was bought from Sigma-Aldrich. Thin films of chitosan were made by spun coated onto standard soda-lime glass microscope slides, (Thermo Scientific). A calibration curve was carried out to identify the spin speed to achieve ~500 nm thick films of chitosan. The films were left for one day to dry before the films were laser ablated. Weight of 0.2 mg of chitosan powder was dissolved in 10 mL acetic acid to obtain a 2% concentration of chitosan solution.

3. Results and Discussion

3.1. Laser Ablation

To determine the laser fluence needed for subsequent laser ablation experiments, etch rate measurements were carried out. Application of the Beer-Lambert law, and using equation (3-1) an ablation threshold of 85 ± 8 mJcm^{-2} and an effective absorption coefficient of 6.4 ×10^4 cm^{-1} was determined. The absorption coefficient of chitosan at visible wavelengths has been widely reported but less so at a wavelength 193nm. Table 1 lists the absorption coefficients, α_{eff}, and α_{trans} corresponding to the effective absorption coefficient from laser etch rate measurements and optical transmission measurements along with their corresponding optical absorption depths.

Table 3-1: The absorption coefficient of chitosan calculated from the etch rate data and from the extension coefficient extracted from the transmission data with corresponding optical absorption depth.

Absorption Coefficient (cm^{-1}) (nm)		Optical Absorption Depth	
α_{eff}	6.4×10^4	α_{eff}^{-1}	155
α_{trans}	3×10^3	α_{trans}^{-1}	3,333

As expected at 193 nm strong optical absorption occurs close to the surface of chitosan. An equation for the etch depth per pulse as a function of the laser fluence, F, is shown in equation (1) below, where F_T is the ablation threshold.

$$d(F) = \frac{1}{\alpha_{eff}} \ln\left(\frac{F}{F_T}\right) \tag{3-1}$$

The etch rate is of the order ~ 10 nm per laser pulse was calculated at a laser fluence close to the ablation threshold, F_T = 100 mJcm^{-2}. Hence, relatively high depth resolution is observed when irradiating chitosan at a wavelength of 193 nm. Optical micrograph of surface relief grating made of chitosan is illustrated in figure 3. It can be noticed that well-defined linear grooves were formed, with little redeposited materials were left on the chitosan film surface.

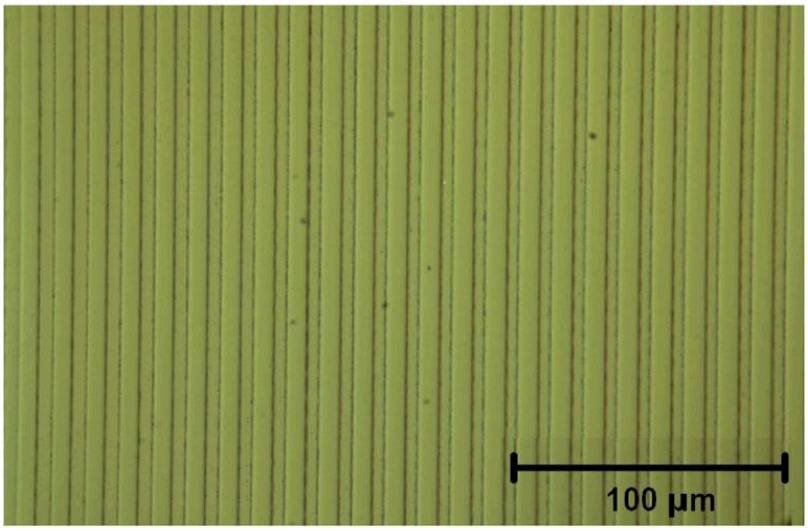

Figure 3: Optical micrograph of a chitosan relief grating fabricated by LDW technique using 193 nm excimer laser. 12 µm grating period, F = 110 mJcm^{-2}, overlapping pulses of 42 pulses and a pulse repetition frequency of 10Hz.

A line profile was extracted from WLI data and a grating period of up to 12 μm was determined. Figure 4 displays a graph of the spatial frequency of the grating. Using WLI measurements, these data were acquired and analysed using the choice Power Spectral Density (PSD). As the PSD result shows, the grating has a well-defined 12 μm length. It is also noted from the graph that one can see a subgrating structure of the ~4 μm and ~6 μm of periodic. This is assumed to be due to stitch errors and the potential relaxation of the surface tension. Figure 4 inset depicts a small grating area in three dimensions.

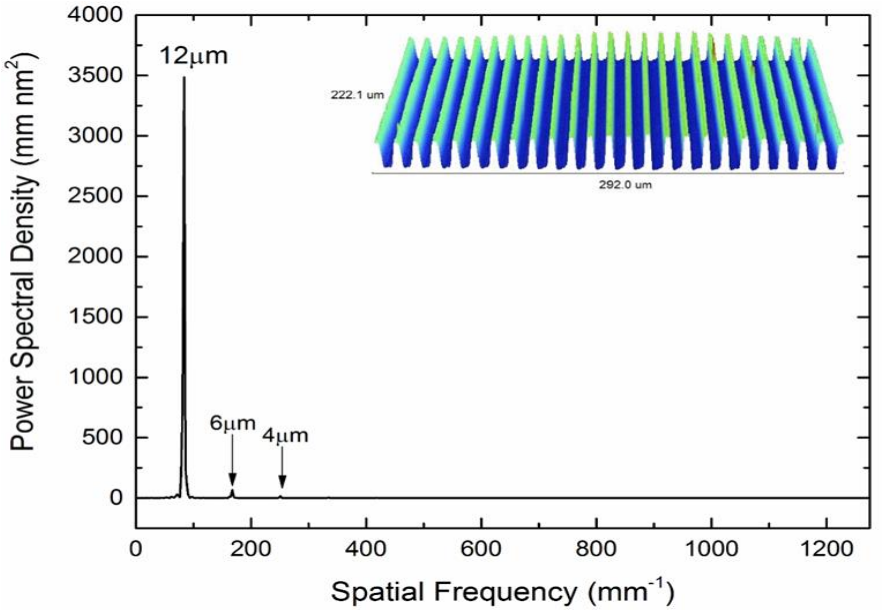

Figure 4: Chitosan grating measured with Power Spectral Density (PSD) using a white light interferometer, 10 × magnification objective lens. Inset displays a 3D image of a small area of the grating.

Figure 5 depicts the one dimension of four surface ridges of the grating. There is some evidence that peak asymmetry is compatible with PSD measurements.

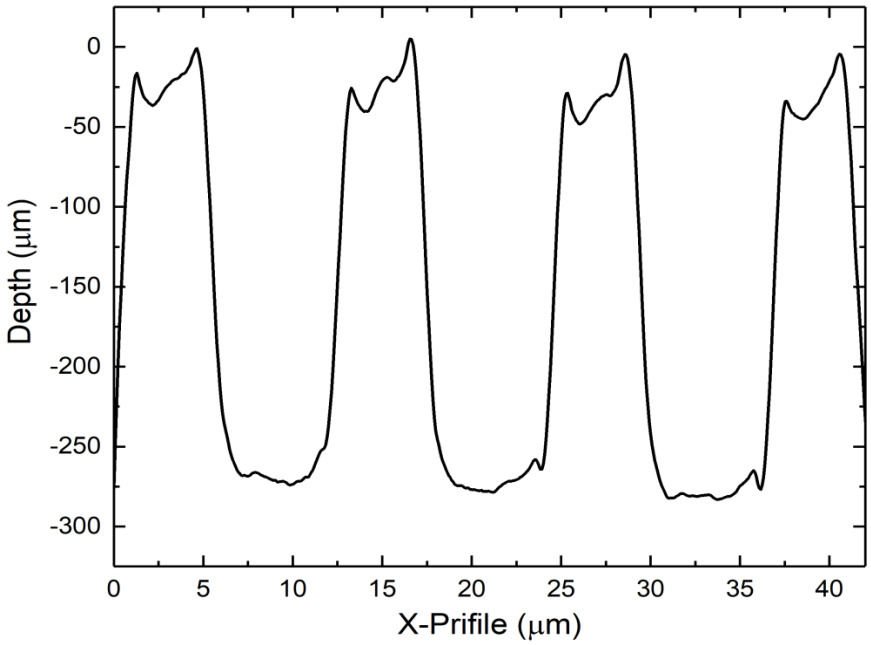

Figure 5: Chitosan surface relief grating cross-section was obtained using white light interferometer data. ~ 250 nm depth was measured.

SEM measurement of the biocompatible chitosan diffraction grating is shown in figure 6. Observation of well-established chitosan tracks at the top of these tracks with some signs of surface texture. The systematic study was conducted using WLI for surface roughness of unirradiated chitosan spun films and chitosan treated with the laser. R_a ~ 4 nm of surface roughness was measured In the as-spun film, while the surface roughness for the chitosan film treated with the laser is slightly increased to be of R_a ~ 6 nm. Masking technique in WLI was used for all surface roughness measurements.

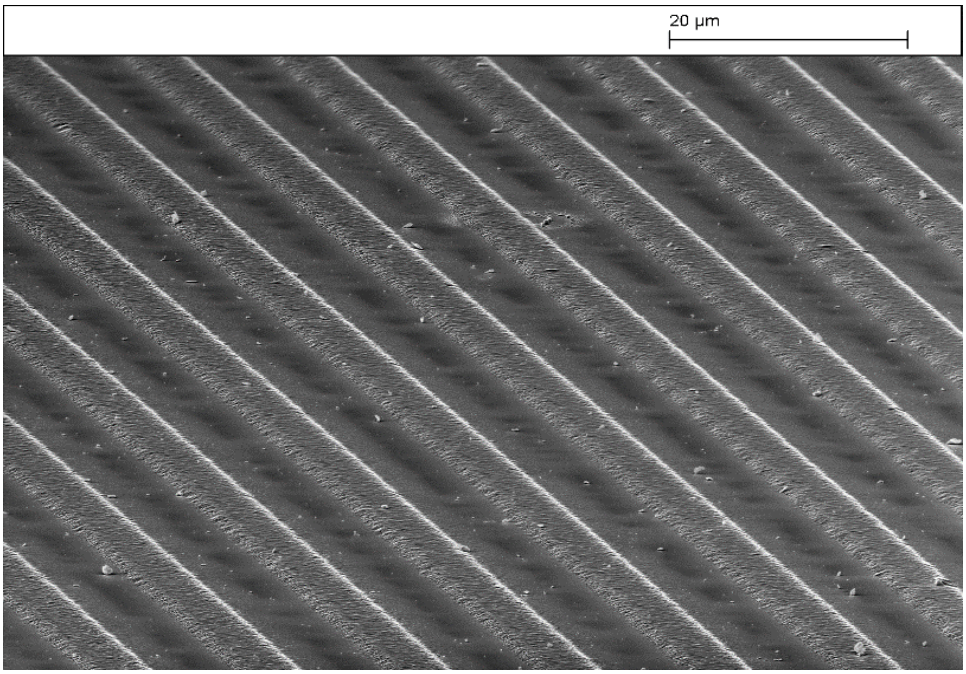

Figure 6: The SEM of surface relief grating of chitosan film (9k × magnifications, 80° tilt). 110mJcm^{-2} laser fluence at a pulse repetition frequency of 10Hz.

To be noticed that the area in which these measurements are obtained over a small area and therefore we should not draw too many conclusions from the measurements of irradiated and unirradiated surface roughness other than spun coated surface roughness is weak and potentially useful for optical components. Ideally, the grating ridges should be voided of 193 nm photon flux during laser processing and thus the texture seen on the ridges may be due to stress-induced relaxation as the chitosan temperature rises and falls. A Fraunhofer intensity pattern created using a HeNe laser light is shown in Figure 7. The 0 and ±1, ±2 diffracted orders are clearly seen in figure 7. By this figure, it can be noticed there are Some scattered between the orders. Efficiencies in the diffraction grating order are measurements. During these measurements, the chitosan films were left on their glass substrates and probed with a HeNe laser with a wavelength of 632.8 nm and a 5 Watt power. The efficiencies between the corresponding positive and negative diffracted orders were symmetrical within the uncertainty associated with the grating measurements: **0** = 40%, **±1** = 24%, **± 2** = 2% (order uncertainty ± 3%, reflection loss 4%). Chitosan laser processing at a wavelength of 193 nm shows the strong effective coupling of UV light with relatively small damage caused by the laser.

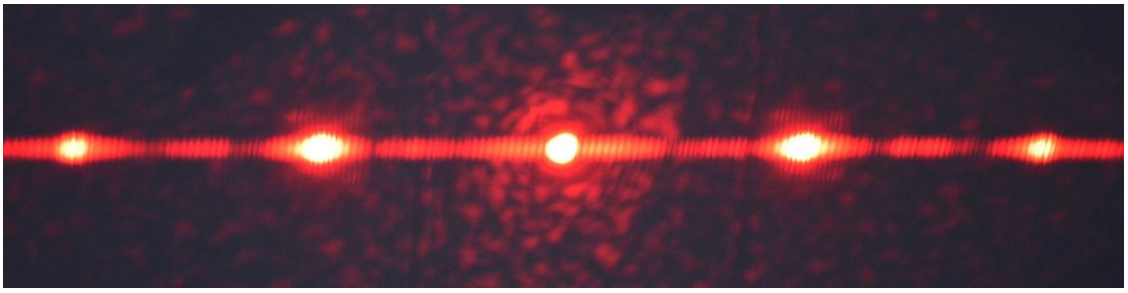

Figure 7: Far-field diffraction pattern of the chitosan grating, lightened with a 5W HeNe laser, wavelength 632.8nm.

The heat diffusion length l_h measurements were limited to a short distance, $l_h = \sqrt{4D\tau}$ = 200 nm. Laser ablation below the ablation threshold was performed to reduce the temperature rise caused during laser ablation.

3.2. Temperature Calculations

Knowledge of the sample, temperature-induced by laser processing provides useful information to interpret ablation experiments. We calculate the surface temperature using equation (3-2) for three different laser fluence [21].

$$T_S(t) = T_0 + \frac{\alpha A}{\rho c}\int_0^t I(t-t')\cdot \exp(\alpha^2 Dt')\cdot erfc\left(\sqrt{\alpha^2 Dt'}\right)dt' \qquad (3\text{-}2)$$

where, I, T_0, α, A, ρ, c, R, D, t, $erfc$ are the laser intensity, initial temperature, absorption coefficient, absorptivity (1-R), mass density, specific heat capacity, reflectivity, thermal diffusivity heat duration

and complimentary error function respectively. The temporal excimer laser pulse shape was simulated using equation (3-3).

$$I(t) = I_0 \cdot \frac{t}{\tau} \cdot \exp\left(\frac{-t}{\tau}\right) \tag{3-3}$$

where τ = 4.5 ns corresponds to the 11.5 ns FWHM laser pulse that was used in these experiments , I_0, is the laser intensity. The simulated laser pulse is shown in the inset of figure 8 and resembles quite well the measured laser pulse. The simplified calculations estimate the surface temperature of chitosan when subjected to a single excimer laser pulse. We assume the thermal and optical properties are temperature independent and we neglect the discrepancies between the gas and condensed phase enthalpies. Also, due to the relatively low laser fluence employed in the experiments we assume, The incident laser pulse is not shielded by the ablated materials. The absorption coefficient used for the temperature calculations of chitosan was from spectrophotometer transmission measurements that exhibited thin film interference effects which were used to extract the extinction coefficient, k = 0.0046 and used in α_{trans} [22,23], see table 1. Calculating the surface temperature at a laser fluence of 90 mJcm^{-2} (ablation threshold) and using the absorption coefficient α = 3 ×10^3 cm^{-1} (α^{-1}~3 μm) corresponds to a calculated surface temperature $T^{90}_{S,\alpha=3\times10^3}$ = 347 K, see Figure 8. We note that the ablation threshold indicates the onset of significant mass removal, and atoms will be removed at a slightly lower laser fluence especially noticeable if a large number of laser pulses are delivered. This region below the laser ablation threshold, say 80 mJcm^{-1}, is also calculated and corresponds to a temperature of $T^{80}_{S,\alpha=3\times10^3}$ = 335 K.

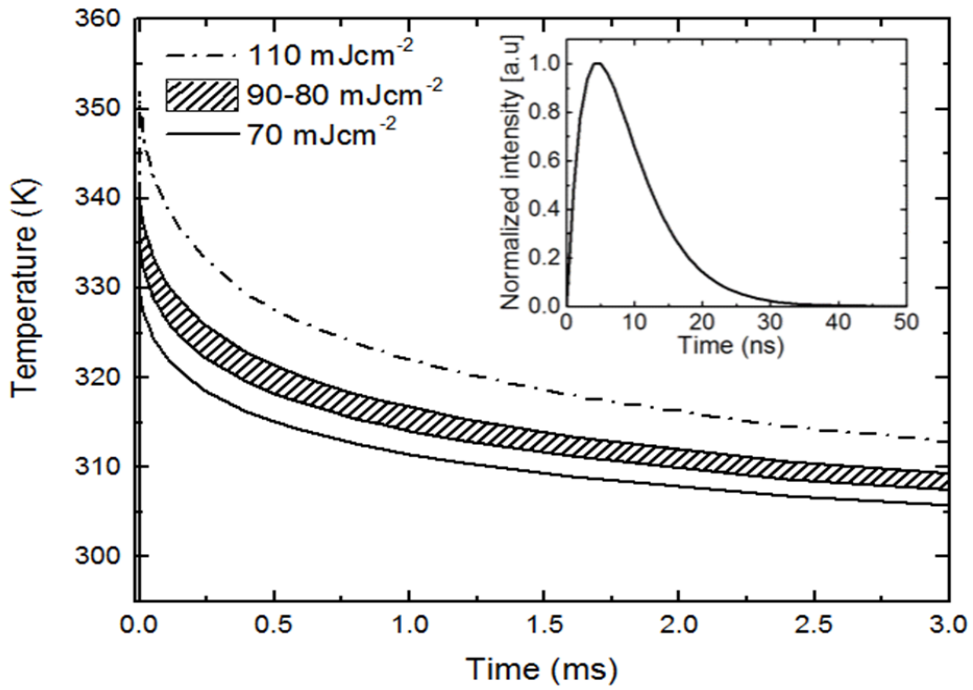

Figure 8:The surface temperature of chitosan sample irradiated at different laser fluence (70 mJcm^{-2},80 mJcm^{-2} , 90 mJcm^{-2}, 110 mJcm^{-2}). The inset shows the simulated laser pulse shape used for the calculations .

The decomposition temperature of bulk chitosan is T_d ~300K obtained from TGA analysis measurements [24]. Using equation (3-2) we calculate the laser fluence that would be necessary to reach the thermos-gravimetric decomposition temperature of chitosan. An estimate of the laser fluence that would be required for chitosan to reach the decomposition temperature is calculated to be in the fluence range of ~ 58-66 mJcm^{-2}. Hence the fluence used in these experiments is consistent with calculations.

4. Discussion

An interesting research area is the laser processing of biocompatible materials. This research was performed primarily to examine the interaction between UV 193 nm laser radiation and chitosan. Secondly, analysis of the surface resolution and feasibility of small optical components. Diffraction gratings are an optical component which could be used on LOC platforms perhaps, as grating couplers or on-chip sensors. Other bio-compatible components could also be fabricated using similar UV laser patterning to produce waveguides and lenses for example and could, therefore, be integrated on board LOC architectures [25–28]. It is therefore envisaged that laser processing could be applied to similar bio-compatible materials and applications. Reducing the grating pitch, for example, to realise bio-compatible distributed feedback lasers [29,30] may be an interesting direction forward. From a material perspective, silk fibroin is another interesting bio-compatible material [31] and the authors of this paper are currently carrying out similar work in this area.

5. Conclusion.

An ArF 193 nm laser was used to realise a spun chitosan thin film diffraction grating. The absorption of chitosan is relatively high at 193 nm wavelength which enables controlled mass removal rates resulting in a high depth resolution processing. We report the ablation threshold for chitosan which is at the sub hundred mJcm^{-2} level. Measurements for optical and SEM indicate clean ablation with limited deposit content. There is some evidence of texture in the laser ablated areas, but there is no substantial evidence that the optical properties of the diffraction grating have affected by the texture. Therefore, the LDW technique should be extended to similar bio-compatible materials.

6. Acknowledgements

We acknowledge the Ministry of Higher Education & Scientific Research, Iraq for supporting Abdulsattar Aesa on a PhD at the University of Hull. Mr Anthony Sinclair is acknowledged for the SEM measurements and Mr David Stavenau is also acknowledged for the technical support.

References

[1] Palmer C. *Diffraction Grating Handbook*. J Opt Soc Am 2005;46:271. doi:10.1364/JOSA.46.000050.
[2] Lenhert S, Brinkmann F, Laue T, Walheim S, Vannahme C, Klinkhammer S, et al. Lipid multilayer gratings. *Nat Nanotechnol* 2010;**5**:275–9. doi:10.1038/nnano.2010.17.
[3] Squires AD, Constable E, Lewis RA. 3D Printed Terahertz Diffraction Gratings And Lenses. J Infrared, Millimeter, Terahertz Waves 2014;**36**:72–80. doi:10.1007/s10762-014-0122-8.
[4] Dyer PE, Maswadi SM, Walton CD, Ersoz M, Fletcher PDI, Paunov VN. 157-nm laser micromachining of N-BK7 glass and replication for microcontact printing. *Appl Phys A Mater Sci Process* 2003;**77**:391–4. doi:10.1007/s00339-002-1936-0.
[5] Hermann S, Shallcross RC, Meerholz K. Simple Fabrication of an Organic Laser by Microcontact Molding of a Distributed Feedback Grating. *Adv Mater* 2014;**26**:6019–24. doi:10.1002/adma.201401616.
[6] Ihlemann J, Müller S, Puschmann S, Schäfer D, Wei M, Li J, et al. Fabrication of submicron gratings in fused silica by F2-laser ablation. *Appl Phys A Mater Sci Process* 2003;**76**:751–3. doi:10.1007/s00339-002-1467-8.
[7] Meinertz J, Fricke-Begemann T, Ihlemann J. Micron and sub-micron gratings on glass by UV laser ablation. *Phys Procedia* 2013;**41**:708–12. doi:10.1016/j.phpro.2013.03.137.
[8] Dyer PE, Farley RJ, Giedl R, Karnakis DM. Excimer laser ablation of polymers and glasses for grating fabrication. *Appl Surf Sci* 1996;**96–98**:537–49. doi:10.1016/0169-4332(95)00528-5.
[9] He PJW, Katis I, Eason RW, Sones CL. Engineering fluidic delays in paper-based devices using laser direct writing. *Lab Chip* 2015:4054–61. doi:10.1039/C5LC00590F.
[10] Waugh DG, Lawrence J. On the use of CO2 laser induced surface patterns to modify the wettability of poly(methyl methacrylate) (PMMA). *Opt Lasers Eng* 2010;**48**:707–15. doi:10.1016/j.optlaseng.2010.01.005.
[11] Lin B, Tjin SC, Wang G, Shum P. High fluence KrF excimer laser fabricated Bragg grating in a microfiber. *Phys. Procedia*, **vol. 19**, 2011, p. 315–8. doi:10.1016/j.phpro.2011.06.167.

[12] Violakis G, Limberger HG, Zlenko AS, Semjonov SL, Bufetov I a, Mashinsky VM, et al. Fabrication of Bragg gratings in microstructured and step index Bi-SiO2 optical fibers using an ArF laser. *Opt Express* 2012;**20**:B118-23. doi:10.1364/OE.20.00B118.
[13] Zhang J, Herman P, Lauer C. 157-Nm Laser-Induced Modification of Fused-Silica Glasses. *Spie* 2001;**4274**:125–32. doi:10.1117/12.432504.
[14] Dubas ST, Iamsamai C, Potiyaraj P. Optical alcohol sensor based on dye-Chitosan polyelectrolyte multilayers. *Sensors Actuators, B Chem* 2006;**113**:370–5. doi:10.1016/j.snb.2005.03.032.
[15] Aldana AA, Barrios B, Strumia M, Correa S, Martinelli M. Dendronization of chitosan films: Surface characterization and biological activity. *React Funct Polym* 2016;**100**:18–25. doi:10.1016/j.reactfunctpolym.2016.01.003.
[16] Xin-Yuan S. New Contact Lens Based on Chitosan/Gelatin Composites. *J Bioact Compat Polym* 2004;**19**:467–79. doi:10.1177/0883911504048410.
[17] Behl G, Iqbal J, O'Reilly NJ, McLoughlin P, Fitzhenry L. Synthesis and Characterization of Poly(2-hydroxyethylmethacrylate) Contact Lenses Containing Chitosan Nanoparticles as an Ocular Delivery System for Dexamethasone Sodium Phosphate. *Pharm Res* 2016;**33**:1638–48. doi:10.1007/s11095-016-1903-7.
[18] Jayakumar R, Reis RL, Mano JF. Chemistry and applications of phosphorylated chitin and chitosan. *E-Polymers* 2006:1–16. doi:035.
[19] Kumar M. A review of chitin and chitosan applications. *React Funct Polym* 2000;**46**:1–27. doi:10.1016/S1381-5148(00)00038-9.
[20] Mironenko AY, Sergeev AA, Nazirov AE, Modin EB, Voznesenskiy SS, Bratskaya SY. H2S optical waveguide gas sensors based on chitosan/Au and chitosan/Ag nanocomposites. *Sensors Actuators, B Chem* 2016;**225**:348–53. doi:10.1016/j.snb.2015.11.073.
[21] Anisimov SI, Luk'yanchuk BS. Selected problems of laser ablation theory. *Physics-Uspekh*i 2002;**45**:293. doi:10.3367/UFNr.0172.200203b.0301.
[22] Manifacier JC, Gasiot J, Fillard JP. A simple method for the determination of the optical constants n, k and the thickness of a weakly absorbing thin film. *J Phys E* 2001;**9**:1002–4. doi:10.1088/0022-3735/9/11/032.
[23] Swanepoel R. Determination of the thickness and optical constants of amorphous silicon. *J Phys E* 2000;**16**:1214–22. doi:10.1088/0022-3735/16/12/023.
[24] Hong PZ, Li SD, Ou CY, Li CP, Yang L, Zhang CH. Thermogravimetric analysis of chitosan. *J Appl Polym Sci* 2007;**105**:547–51. doi:10.1002/app.25920.
[25] Lawrence BD, Cronin-Golomb M, Georgakoudi I, Kaplan DL, Omenetto FG. Bioactive silk protein biomaterial systems for optical devices. *Biomacromolecules* 2008;**9**:1214–20. doi:10.1021/bm701235f.
[26] Vörös J, Ramsden JJ, Csúcs G, Szendro I, De Paul SM, Textor M, et al. Optical grating coupler biosensors. *Biomaterials* 2002;**23**:3699–710. doi:10.1016/S0142-9612(02)00103-5.
[27] Tiefenthaler K. Grating couplers as label-free biochemical waveguide sensors. *Biosens Bioelectron* 1993;**8**:6–8. doi:10.1016/0956-5663(93)80070-6.
[28] Pantelic D, Savic S. Biopolymer holographic diffraction gratings 2008;30:1205–7. doi:10.1016/j.optmat.2007.05.056.
[29] Barbosa-silva R. Silk fibroin biopolymer films as efficient hosts for DFB laser operation 2013:7181–90. doi:10.1039/c3tc30903g.
[30] Toffanin S, Kim S, Cavallini S, Natali M, Benfenati V, Amsden JJ, et al. Low-threshold blue lasing from silk fibroin thin films 2012;091110. doi:10.1063/1.4748120.
[31] Amsden JJ, Domachuk P, Gopinath A, White RD, Negro LD, Kaplan DL, et al. Rapid nanoimprinting of silk fibroin films for biophotonic applications. *Adv Mater* 2010;**22**:1746–9. doi:10.1002/adma.200903166.